10 per cent or less over the 27 db range in incident local oscillator power level. The total change in shunt capacity over the same range operating in the optimum bias condition was also considerably less than in the zero bias condition.

The general characteristic of reduction of signal sensitivity by decreasing or increasing the bias from the optimum condition, as is demonstrated in Figs. 1–5, points to another possible application of the biased mixer diode. Although not shown in these figures, the application of a backward bias (negative values of the abscissas in Figs. 1–5) causes a smooth decrease in signal sensitivity as the bias goes through zero into the negative region. These same trends hold at high signal levels, that is, the bias controls either the high signal level or low signal level conversion loss. If the mixer diode has a positively or negatively polarized feedback AGC type of signal applied when operating at optimum dc bias, or a negatively polarized feedback signal when operating at zero dc bias, signal limiting could be achieved at the input to the first IF stage. This could be done only at high signal levels; otherwise the reduction in signal to noise ratio would deteriorate low signal level performance. However, at high incident signal levels a reduction of S/N is tolerable. Thus at high signal levels this type of automatic signal limiting would serve as a supplementary adjunct to a conventional AGC, the automatic signal-limiting bias being developed at a lower level, say after only a few stages of amplification. This would keep the lower level amplifiers from saturating at high incident RF signal levels and thereby extend the effective AGC range. Whether the signal distortion introduced by the accompanying changes in equivalent mixer R_p and C_p would be more or less than that caused by amplifier saturation would have to be determined.

Conclusions

The experimental observations disclosed that:

1) The optimum bias for a particular type of diode varies little from diode to diode within a type.
2) The optimum bias is independent of signal or L.O. frequency.
3) There is a large tolerance, percentagewise, in the vicinity of optimum bias where the resultant tangential signal sensitivity is reduced by only about 1 db for 10 db reduction (from rated values) in local oscillator power.

These results lead to the inference that the use of optimum dc bias as a control feature in mixer design applications should be quite practical.

One to five specimens of several diode types, chosen merely because they were available, all demonstrated that a particular dc bias makes the RF and IF impedances practically stationary with respect to local oscillator power changes. These results suggest to the author that this may be a universal characteristic of mixer diodes that, to his knowledge, has not been heretofore observed.

Acknowledgment

The author wishes to extend his appreciation to Dr. W. H. Watson, who, though not having witnessed the experiments, has shown active interest in the significance of the experimental observations.

Phase, Attenuation, and Impedance Characteristics of Coaxial Transmission Lines with Thin Tubular Conductors*

E. J. POST†

Summary—**The phase, attenuation, and impedance characteristics of coaxial lines are discussed in some detail, stressing the improvements which can be obtained by removing conductor material that is not effective in the main part of the frequency interval for which the line is used. The ensuing attenuation is higher for the low frequencies but lower for the high frequencies, in comparison with the solid conductor line. The corresponding phase (that is, total phase minus the constant delay) is substantially more linear than for solid conductor lines in the frequency interval of interest. The real part of the characteristic impedance is more independent of frequency than for the solid conductor case. The reactive part of the characteristic impedance increases faster for low frequencies, but can be very nearly represented by a pure capacity, thus enabling a more ideal and simple line termination with lumped elements.**

* Received August 30, 1962; revised manuscript received November 19, 1962. Electromagnetic Radiation Laboratory, Project No. 5635. Air Force Cambridge Research Labs., Office of Aerospace Research, U. S. Air Force, L. G. Hanscom Field, Mass.

† Air Force Cambridge Research Laboratories, L. G. Hanscom Field, Bedford, Mass.

I. Introduction

A COMPLETE field treatment of this transmission line as a boundary value problem is very cumbersome because of the complexity of matching boundaries in multiple adjacent regions of different material, requiring the solution of a set of simultaneous transcendental equations. The subject matter commonly encountered in textbooks is the framework of the analysis combined with a discussion of the most conspicuous engineering approximations. It is one of these engineering cases which will be submitted here to a closer examination because it is believed to have some attractive features which might be of interest in current applications.

The transmission improvements in thin tubular conductor transmission lines were probably first mentioned by Carson and Mead; relevant details are dispersed in a number of U. S. patents.[1] Published experimental evidence of the transmission characteristics of these lines was probably given first by Tear and Schatz[2] in 1944, who measured the attenuation as a function of frequency. They found that the attenuation in the range of high frequencies was lower than in the solid conductor case, an effect then somewhat unexpected even though predicted theoretically.

There is, to the best of our knowledge, no experimental material which explicitly confirms that the nonlinear distortion in phase is likewise smaller than for solid conductors, as predicted by Carson and Mead. The distortion component in the phase of transmission lines is a subject that is very much neglected experimentally. This neglect is justifiable somewhat if one has absolute faith in the possible reconstruction of phase from attenuation data. We believe that this reconstruction is possible. Nevertheless, more ample experimental information should be welcomed as a check on the applicability of the phase and attenuation relations, which in turn are needed to check the validity of the engineering approximations of the field approach.

It will not be necessary here to go through all the fundamental equations of transmission line theory. For the present purpose, reference is made to Morgan's[3] treatment of the Clogston line. The introductory part of Morgan's treatment is particularly suited for a discussion of the present case. The Clogston line represents a rather drastic and revolutionary proposal to improve transmission characteristics by modifying wall (or surface) impedances of the conductors. The tubular conductor can be considered, for theoretical purposes, as a degenerate case of the Clogston-type conductor. The simple tubular conductor, however, has the advantage that its practical realization is not beset with so many constructional difficulties as the Clogston-type conductor. The discussion in this paper is in essence an adaptation of Morgan's treatment for engineering approximations relevant to the tubular conductor.

[1] U. S. Patent Nos. 1, 817, 964; 1,972,877; 2,052,317.

[2] B. R. Teare and T. R. Schatz "Copper-covered steel wire at radio frequencies," Proc. IRE, vol. 32, pp. 397–403; July, 1944.

[3] S. P. Morgan, "Laminated transmission lines," *Bell Sys. Tech. J.*, vol. 31, p. 833; 1952.

II. Surface Impedances

The phase and attenuation characteristics of waveguide structures are primarily determined by three factors:

1) The geometry of the guide associated with the choice of transmission mode.
2) The electrical characteristics of the surfaces which constitute the geometry.
3) The electrical characteristics of the transmission medium itself (that is, the dielectric).

For a fixed mode and geometry one may observe that in a first approximation, the expressions for attenuation and phase are made up of additive contributions proportional, respectively, to the real and imaginary part of the impedance ratio

$$\frac{Z_{\text{wall (surface)}}}{Z_{\text{transmission medium}}}, \tag{1}$$

taken for all the surfaces.

The first-order phase and attenuation expressions for the coaxial line (TEM mode) can be written to demonstrate this feature. (See formulas 44 and 45, on page 894 of Morgan[3])

$$\alpha = \frac{\text{Re } Z_1/Z}{2\rho_1 \ln \rho_2/\rho_1} + \frac{\text{Re } Z_2/Z}{2\rho_2 \ln \rho_2/\rho_1} \tag{2}$$

$$\beta = \omega\sqrt{\epsilon\mu} + \frac{\text{Im } Z_1/Z}{2\rho_1 \ln \rho_2/\rho_1} + \frac{\text{Im } Z_2/Z}{2\rho_2 \ln \rho_2/\rho_1}, \tag{3}$$

ρ_1 = radius, inner conductor,
ρ_2 = radius, outer conductor,
Z_1 = surface impedance, inner conductor,
Z_2 = surface impedance, outer conductor,
ϵ = permittivity of transmission medium,
μ = permeability of transmission medium,
$Z = \sqrt{\mu/\epsilon}$ = intrinsic impedance of transmission medium,
ω = frequency $\times 2\pi$.

The range of validity of expressions in (2) and (3) as a function of frequency is primarily determined by the correctness of the expressions which one inserts for Z_1, Z_2, and Z, except for a very-low-frequency restriction which will be discussed in Section IV.

Physically, the design problem of any guide is to optimize the ratio of the energy propagating in the axial direction of the guide to the energy emerging radially into the walls. This aim, roughly speaking, can be approximated by raising $Z_{\text{transmission}}$ and lowering Z_{wall}.

A high $Z_{\text{transmission}}$ can be approached by low ϵ and high μ materials. The limitations of high μ materials for this purpose are too well known to discuss them any

further at this instance. So far, the empty space ϵ and μ are best for a lossless and high transmission impedance; that is,

$$Z = \sqrt{\frac{\mu_0}{\epsilon_0}} = 377 \text{ ohms.} \tag{4}$$

The Z_{wall} in almost all transmission lines and guides in actual use is determined by the intrinsic impedance of the bulk conductor, that is,

$$Z_{\text{wall}} = \sqrt{\frac{\omega\mu}{2\sigma}}(1+j), \tag{5}$$

where σ = conductivity of the wall material and μ = permeability of the wall material.

As a comparison, for copper

$$\begin{aligned} \sqrt{\frac{\omega\mu}{2\sigma}} &\approx 2.6\,10^{-4} \text{ ohm at 1 Mc} \\ \sqrt{\frac{\omega\mu}{2\sigma}} &\approx 2.6\,10^{-2} \text{ ohm at } 10^4 \text{ Mc.} \end{aligned} \tag{6}$$

Hence, even for extremely high frequencies and relatively poor conductors,

$$\left| \frac{Z_{\text{wall}}}{Z_{\text{transmission}}} \right| \ll 1. \tag{7}$$

The objectionable feature of this Z_{wall} is that the real and imaginary parts are both proportional to $\sqrt{\omega}$, which happens to be incompatible with a constant amplitude and low dispersion device. The devout wish of the communication engineer is

$$\begin{aligned} &\text{Re } Z_{\text{wall}} = \text{independent of } \omega \text{ and low,} \\ &\text{Im } Z_{\text{wall}} = \text{proportional to } \omega \text{ (and not } \sqrt{\omega}). \end{aligned} \tag{8}$$

The fact that the amplitude and dispersion of the axial wave depend on the response of the wall to the radially emerging wave strongly suggests a further analysis of the wall impedance. The simplest conceivable structures in this connection are (thin) conducting layers backed (terminated) by another material, with different electrical characteristics, as illustrated in Fig. 1.

The surface impedance Z_s of a simple composite surface as given in Fig. 1, is according to standard theory[4]

$$Z_s = \frac{1 - re^{-2\gamma t}}{1 + re^{-2\gamma t}} Z_c, \tag{9}$$

where γ is the propagation parameter of material ①, Z_c its intrinsic or characteristic impedance and r the reflection coefficient in the "four terminal section" ① of thickness t. The terminating impedance represented by material ② is given as Z_t; the reflection coefficient is then known to be

$$r = \frac{Z_c - Z_t}{Z_c + Z_t}. \tag{10}$$

The real advantage of using the so-called canonical four terminal parameters, γ and Z_c, rather than the equivalent circuit parameters is that both of these can be more conveniently and simply expressed in the material constants σ, μ and ϵ, which are the parameters physically available for the design.

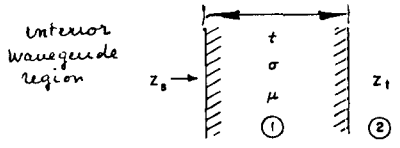

Fig. 1—Surface coating material ①. Conductivity σ, permeability μ, on base material ②, representing terminating impedance Z_t.

The relations expressing γ and Z_c in the material constants are known to be

$$\gamma = \sqrt{\frac{\omega\mu\sigma}{2}}(1+j) \tag{11}$$

$$Z_c = \sqrt{\frac{\omega\mu}{2\sigma}}(1+j). \tag{12}$$

Both are complex with phase angles $\pi/4$, which is characteristic for any conductor in the frequency range where conduction current prevails over displacement current; that is,

$$\sigma \gg |j\omega\epsilon|. \tag{13}$$

The inequality equation (13) still holds for metals in the range of optical frequencies.

Another known restriction for (11) and (12) is that the radius ρ of surface curvature should be large with respect to the so-called skin depth, given by the reciprocal value of the factor in γ; that is,

$$\rho \gg \sqrt{\frac{2}{\omega\mu\sigma}}. \tag{14}$$

The inequality (14) of course breaks down for low frequencies. But for thin layers the current is substantially confined to the thickness of the layer, and (14) can then be replaced by

$$\rho \gg t. \tag{14a}$$

Now the real and imaginary parts of the impedance function Z_s as given by (9) for different reflection coefficients r, (10), will be evaluated. This reflection coefficient is real if a metal coating is backed by another metal layer thick enough so that Z_t may be taken as the intrinsic impedance of this second metal. Then r, in principle, lies between -1 to $+1$; that is,

$$-1 \leq r \leq +1. \tag{15}$$

[4] See for instance, S. Ramo and J. R. Whinnery, "Fields and Waves in Modern Radio," John Wiley and Sons, Inc., New York, N. Y. Eq. (9) is implied by the explanations in Article 6.10.

For another case of engineering interest, namely a conductor ① enclosing an essentially lossless dielectric ②, Z_t is very large, and r is effectively real, -1. It is convenient for the decomposition of Z_s into real and imaginary parts to introduce r as an exponential. This requires that two cases be distinguished.

$$0 \geq r \geq -1 \qquad r = e^{-\xi - \pi i} = -e^{-\xi} \tag{16}$$

$$0 \geq r \geq +1 \qquad r = e^{-\xi} \qquad \text{for } \xi = 0 \to \infty. \tag{17}$$

The real and imaginary parts of Z_s for the reflection coefficient intervals in (16) and (17) are then

$$0 \geq r \geq -1 \begin{cases} \operatorname{Re} Z_s = \dfrac{\sinh(2\bar{\gamma}t + \xi) + \sin 2\bar{\gamma}t}{\cosh(2\bar{\gamma}t + \xi) - \cos 2\bar{\gamma}t} \cdot \sqrt{\dfrac{\omega\mu}{2\sigma}} \\ \\ \operatorname{Im} Z_s = \dfrac{\sinh(2\bar{\gamma}t + \xi) - \sin 2\bar{\gamma}t}{\cosh(2\bar{\gamma}t + \xi) - \cos 2\bar{\gamma}t} \cdot \sqrt{\dfrac{\omega\mu}{2\sigma}} \end{cases} \tag{18}$$

with

$$\bar{\gamma} = \sqrt{\frac{\omega\mu\sigma}{2}}$$

$$0 \leq r \leq +1 \begin{cases} \operatorname{Re} Z_s = \dfrac{\sinh(2\bar{\gamma}t + \xi) - \sin 2\bar{\gamma}t}{\cosh(2\bar{\gamma}t + \xi) + \cos 2\bar{\gamma}t} \cdot \sqrt{\dfrac{\omega\mu}{2\sigma}} \\ \\ \operatorname{Im} Z_s = \dfrac{\sinh(2\bar{\gamma}t + \xi) + \sin 2\bar{\gamma}t}{\cosh(2\bar{\gamma}t + \xi) + \cos 2\bar{\gamma}t} \cdot \sqrt{\dfrac{\omega\mu}{2\sigma}}. \end{cases} \tag{19}$$

For design purposes, one likes to see these expressions as functions of ω. The argument $\bar{\gamma}t$ together with (11) thus suggests the definition,

$$\sqrt{\Omega} = 2\bar{\gamma}t$$

or

$$\Omega = 2\omega\mu\sigma t^2 \tag{20}$$

where Ω is a dimensionless reduced frequency proportional to the actual frequency.

The factor $\sqrt{\omega\mu/2\sigma}$, which stems from the characteristic impedance Z_c given by (12), can be expressed in the reduced frequency defined by (20) as

$$\sqrt{\frac{\omega\mu}{2\sigma}} = \sqrt{\frac{\mu}{2\sigma}\,\frac{\Omega}{2\mu\sigma t^2}} = \frac{1}{2\sigma t}\sqrt{\Omega}. \tag{21}$$

Substitution of (20) and (21) into (18) and (19) yields the following set of functions:

$$0 \geq r \geq -1 \begin{cases} \operatorname{Re} Z_s = \sqrt{\Omega}\,\dfrac{\sinh(\xi + \sqrt{\Omega}) + \sin\sqrt{\Omega}}{\cosh(\xi + \sqrt{\Omega}) - \cos\sqrt{\Omega}}\,\dfrac{1}{2\sigma t} \\ \\ \operatorname{Im} Z_s = \sqrt{\Omega}\,\dfrac{\sinh(\xi + \sqrt{\Omega}) - \sin\sqrt{\Omega}}{\cosh(\xi + \sqrt{\Omega}) - \cos\sqrt{\Omega}}\,\dfrac{1}{2\sigma t} \end{cases} \tag{22}$$

$$0 \leq r \leq 1 \begin{cases} \operatorname{Re} Z_s = \sqrt{\Omega}\,\dfrac{\sinh(\xi + \sqrt{\Omega}) - \sin\sqrt{\Omega}}{\cosh(\xi + \sqrt{\Omega}) + \cos\sqrt{\Omega}}\,\dfrac{1}{2\sigma t} \\ \\ \operatorname{Im} Z_s = \sqrt{\Omega}\,\dfrac{\sinh(\xi + \sqrt{\Omega}) + \sin\sqrt{\Omega}}{\cosh(\xi + \sqrt{\Omega}) + \cos\sqrt{\Omega}}\,\dfrac{1}{2\sigma t}. \end{cases} \tag{23}$$

The functions in the right-hand members of (22) and (23), preceding the common factor $1/2\sigma t$, present four single parameter families of curves with argument Ω. They have been tabulated and the results are shown in Figs. 2 and 3. The parameter ξ has been reconverted into the reflection coefficient r so that the real and imaginary parts of Z_s in (18) and (19), respectively, can be combined in one family with parameter r between -1 and $+1$.

It should be noted that these curves for metal layers oscillate around the curve for $r=0$. For large argument Ω, all of them asymptotically approach the curves for $r=0$. The reflection coefficient, zero, corresponds to the behavior of a solid conductor, because $Z_c=Z_t$ can be effected by backing a metal layer by a metal with the same electrical characteristics. To emphasize the possibilities of linear phase behavior, it has been thought desirable to plot the curves on a linear rather than on the usual logarithmic scale.

III. Practical Possibilities for a Reflection Coefficient $r=-1$

Recalling the structure of the attenuation and phase formulas for a coaxial line given by (2) and (3), it should be clear that Figs. 2 and 3 immediately give the relative behavior of α and β. If both conductors are the same electrically, then Fig. 2 gives the true α of the cable except for a constant of proportionality, provided the transmission medium (dielectric) itself is sufficiently

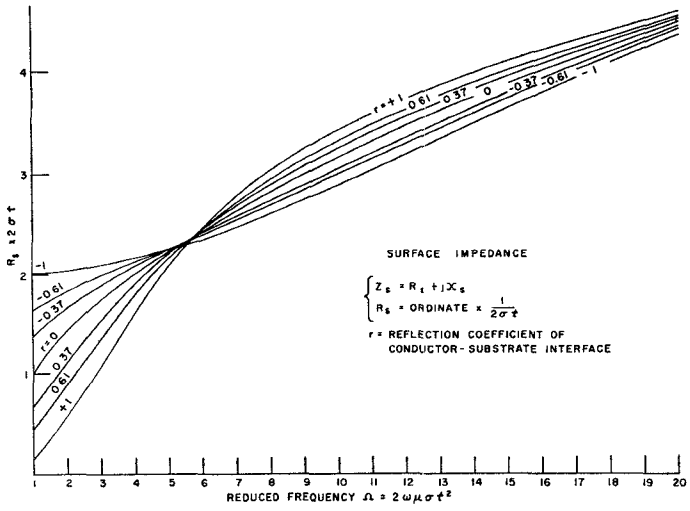

Fig. 2—Resistive part of surface impedance Z_s as a function of reduced frequency Ω.

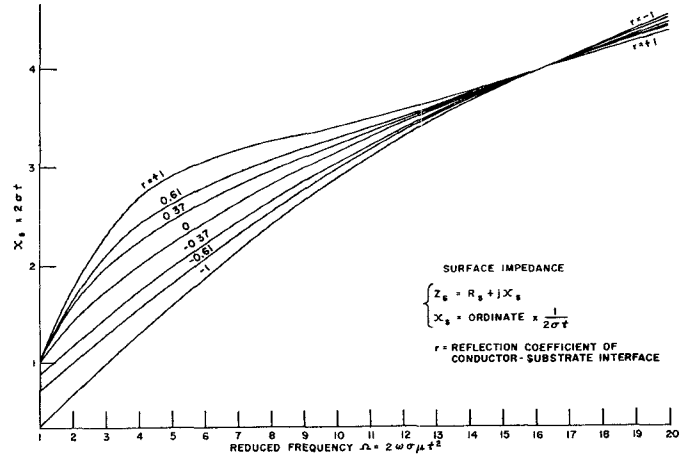

Fig. 3—Reactive part of surface impedance Z_s as a function of reduced frequency Ω.

lossless. The same is true for the phase response. Fig. 3 gives the relative phase due to the influence of the wall. The total phase delay then is obtained by adding the linear contribution already associated with the length of the cable.

A quick look at Figs. 2 and 3 shows that a reflection coefficient $r = -1$ comes fairly close to meeting the design requirements laid down in (8). The phase stays quite linear up to $\Omega = 8$ to 10. For a highest frequency of 10^7 cps this corresponds, according to (20), to a layer thickness of the order of 1 mil for copper. For the same frequency of 10^7 cps (see Fig. 2), R_s is lower than the R_s of a solid copper conductor ($r = 0$).

A reflection coefficient -1, according to (10), requires a terminating impedance Z_t much larger than the characteristic impedance of the surface layer; that is,

$$\left|\frac{Z_t}{Z_c}\right| \gg 1. \tag{24}$$

For an electrically sufficiently thick termination, Z_t may be taken as the intrinsic impedance of material 2 in Fig. 1. The ratio then, according to (5) or (12), becomes

$$\left|\frac{Z_t}{Z_c}\right| = \sqrt{\frac{\mu_2\sigma_1}{\mu_1\sigma_2}}. \tag{25}$$

For μ_1, σ_1 and μ_2, σ_2 the permeabilities and conductivities of copper and iron, respectively, this ratio can be of the order

$$\frac{Z_{\text{iron}}}{Z_{\text{copper}}} \approx 500, \tag{26}$$

thus corresponding to an r very close to -1.

The high permeability substrate material is more specifically useful for the outer conductor of a coaxial line because it quenches the outside field and consequently reduces cross talk and proximity effects for low frequencies.

Another possibility for obtaining a high impedance termination more specifically applicable to the inner conductor, can be effected by means of a dielectric. A dielectric usually has to be very thick before it shows anything like its intrinsic impedance. A solid dielectric rod, however, has a very high impedance in its radial direction for frequencies below the cutoff frequencies of the waveguide modes which it can support if surrounded by a tubular conductor. It should be noted that the insertion of another metal wire embedded in the dielectric inside the tubular conductor (to provide, for example, strength or a low resistance path for repeater power) would disturb this situation because of the creation of a second TEM transmission path.

IV. Characteristic Impedance and Asymptotic Behavior

Now the expressions obtained for the surface impedances will be used in the evaluation of a transmission line. It will be useful, and close to practical possibilities, to assume that the surface impedances of the inner and outer conductors are the same, and that the interface reflection coefficient r between conductor and high impedance substrate is -1. Hence,

$$Z_1 = Z_2 = Z_s \qquad (\text{with } r = -1)$$

$$\text{Re } Z_s = \sqrt{\Omega}\,\frac{\sinh\sqrt{\Omega} + \sin\sqrt{\Omega}}{\cosh\sqrt{\Omega} - \cos\sqrt{\Omega}}\,\frac{1}{2\sigma t}$$

$$\text{Im } Z_s = \sqrt{\Omega}\,\frac{\sinh\sqrt{\Omega} - \sin\sqrt{\Omega}}{\cosh\sqrt{\Omega} - \cos\sqrt{\Omega}}\,\frac{1}{2\sigma t}. \tag{27}$$

Furthermore, it is convenient to introduce a special symbol for the geometric factor in the phase and attenuation expressions in (2) and (3).

$$\frac{1}{\rho} = \frac{\left(\frac{1}{\rho_1} + \frac{1}{\rho_2}\right)}{2\ln\rho_2/\rho_1}. \tag{28}$$

The expressions for attenuation and phase can then be written in the simple form

$$\alpha = \frac{\operatorname{Re} Z_s}{\rho\sqrt{\frac{\mu}{\epsilon}}}$$

$$\beta = \omega\sqrt{\epsilon\mu} + \frac{\operatorname{Im} Z_s}{\rho\sqrt{\frac{\mu}{\epsilon}}}. \tag{29}$$

The wave impedance Z in the axial direction is the quotient of the radial electric field and azimuthal magnetic field. This ratio according to formula (33) in Morgan's paper[3] is

$$Z_w = \frac{\gamma}{j\omega\epsilon} \qquad (\text{with } \gamma = \alpha + j\beta), \tag{30}$$

if the conductivity of the medium between the conductors is zero. Expressed in the (dimensionless) reduced frequency Ω defined by (20), the real and imaginary parts become

$$\operatorname{Re} Z_w = \sqrt{\frac{\mu}{\epsilon}}\left\{1 + \frac{2\sigma t \operatorname{Im} Z_s}{\Omega}\frac{t}{\rho}\right\}$$

$$\operatorname{Im} Z_w = \sqrt{\frac{\mu}{\epsilon}}\frac{2\sigma t \operatorname{Re} Z_s}{\Omega}\frac{t}{\rho}. \tag{31}$$

For the derivation of (31) from (30), it has been assumed that the conductors and the medium between the conductors have the same permeability.

The characteristic impedance Z_c of the line itself can now safely be obtained from (31) by means of the common formula

$$Z_c = \frac{\ln \rho_2/\rho_1}{2\pi} Z_w, \tag{32}$$

because, as mentioned earlier, Z_w is exact. Eqs. (29) and (32) for a thin conductor line have been plotted in Figs. 4–7 to show the over-all performance in comparison with a solid conductor line of the same dimensions.

The asymptotic behavior of (29) and (31) for high and low frequencies depends very much on the behavior of Z_s. One finds

$$\lim_{\Omega\to\infty} \operatorname{Re} Z_s = \frac{\sqrt{\Omega}}{2\sigma t}$$

$$\lim_{\Omega\to\infty} \operatorname{Im} Z_s = \frac{\sqrt{\Omega}}{2\sigma t} \tag{33}$$

and

$$\lim_{\Omega\to 0} \operatorname{Re} Z_s = \frac{1}{\sigma t}$$

$$\lim_{\Omega\to 0} \operatorname{Im} Z_s = \frac{\Omega}{3}\frac{1}{2\sigma t}. \tag{34}$$

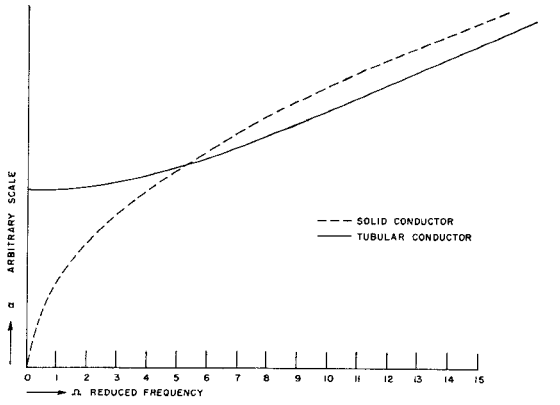

Fig. 4—Comparison of the attenuation of a solid conductor and a tubular conductor transmission line.

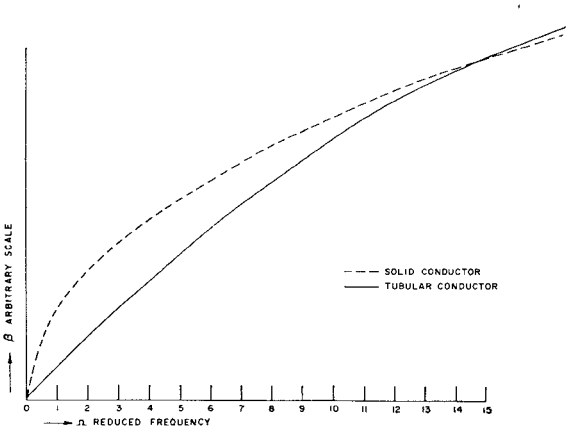

Fig. 5—Comparison of the phase response of a solid conductor and a tubular conductor transmission line.

The high-frequency approximations in (33) clearly lead to the conventional formulas for a solid conductor line with a well-developed skin effect. For attenuation, phase, and impedance, one finds as high-frequency approximations, by substituting (33) into (29) and (31):

$$\alpha = \frac{\sqrt{\Omega}}{2\sigma l\rho\sqrt{\frac{\mu}{\epsilon}}};$$

$$\beta = \omega\sqrt{\epsilon\mu} + \frac{\sqrt{\Omega}}{2\sigma l\rho\sqrt{\frac{\mu}{\epsilon}}} \tag{35}$$

$$\operatorname{Re} Z_w = \sqrt{\frac{\mu}{\epsilon}}\left(1 + \frac{1}{\sqrt{\Omega}}\frac{t}{\rho}\right);$$

$$\operatorname{Im} Z_w = \sqrt{\frac{\mu}{\epsilon}}\frac{1}{\sqrt{\Omega}}\frac{t}{\rho}. \tag{36}$$

The low-frequency approximations are similarly obtained by substituting (34) into (29) and (31):

$$\alpha = \frac{1}{\sigma l\rho\sqrt{\frac{\mu}{\epsilon}}};$$

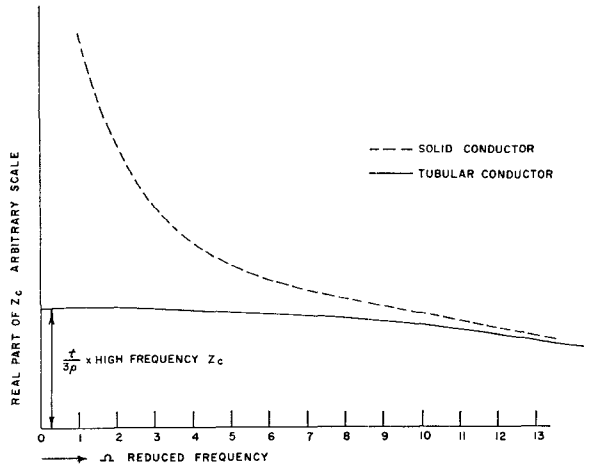

Fig. 6—Comparison between the resistive parts of the characteristic impedance of a transmission line with solid conductors and a transmission line with tubular conductors (zero level high-frequency value).

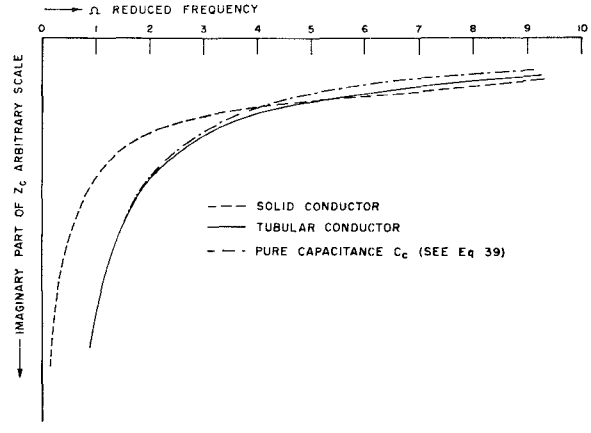

Fig. 7—Reactive parts of the characteristic impedance of a transmission line with solid conductors and a transmission line with tubular conductors in comparison with a pure capacitive reactance.

$$\beta = \omega\sqrt{\epsilon\mu} + \frac{\Omega}{6\sigma t\sqrt{\frac{\mu}{\epsilon}}} \tag{37}$$

$$\text{Re } Z_w = \sqrt{\frac{\mu}{\epsilon}}\left(1 + \frac{1}{3}\frac{t}{\rho}\right);$$

$$\text{Im } Z_w = \sqrt{\frac{\mu}{\epsilon}}\frac{2}{\Omega}\frac{t}{\rho}. \tag{38}$$

Note that α and Re Z_w in (37) and (38) are constants; the latter is almost equal to $\sqrt{\mu/\epsilon}$, because t/ρ as a rule is very small. The phase constant β has only a linear correction term, implying that the propagation velocity is slowed down with respect to the wave velocity $(\epsilon\mu)^{-1/2}$, while Im Z_w is seen to behave as a pure capacitance for $\Omega \to 0$. The reactive part of Z_c can therefore also be represented by a capacity C_c, so that Im $Z_c = 1/\omega C_c$. For the value of C_c, one finds through (20), (28), and (32) that

$$C_c = \sigma\sqrt{\epsilon\mu}\, t\left(\frac{4\pi\rho_1\rho_2}{\rho_1 + \rho_2}\right). \tag{39}$$

For the commonly used diameters of coaxial cables and a copper conductor with a thickness of the order of $t = 0.01$ mm, (39) yields a capacity of the order of a few 0.01 μf. The capacitance given by (39) should be a constant within reasonable limits up to values of Ω for which Im Z_s is still substantially linear. From Fig. 3 for $r = -1$, it is seen that $\Omega = 10$ may be taken as an acceptable upper limit. The deviation between an RC termination as prescribed by (38) and (39), and the actual Z_c of a thin conductor is explicitly shown in Fig. 7. The deviation is seen to become very small for the low frequencies where it counts most. Hence for $\Omega < 10$, one may expect a somewhat improved reflectionless termination by using as representation for Z_c, the following equivalent circuit:

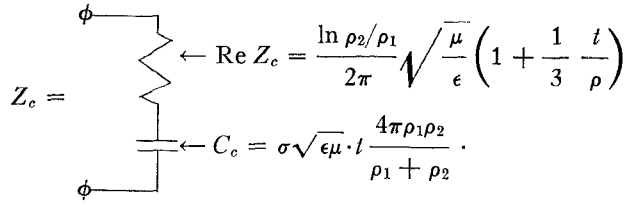

The constant α in the low-frequency approximation in (37) implies that the conductor is uniformly penetrated by the current, thus suggesting that the resistance per unit length in the lumped circuit approximation can be expressed by the dc value

$$R = \frac{1}{2\pi\sigma t}\left(\frac{1}{\rho_1} + \frac{1}{\rho_2}\right). \tag{40}$$

The attenuation in the lumped circuit approach is known to be

$$\alpha \text{ lumped} = \frac{R}{2}\sqrt{\frac{C}{L}}, \tag{41}$$

if

$$R \ll \omega L. \tag{42}$$

Inserting (40) and the usual expressions $L = \mu/2\pi \ln(\rho_2/\rho_1)$ and $C = 2\pi\epsilon/\ln(\rho_2/\rho_1)$ into (41), one finds that

$$\alpha \text{ lumped} = \alpha \tag{43}$$

as defined by (37), if one uses (28) for $1/\rho$.

The curious thing about this identification, (43), is that α lumped, in a sense, stems from a high-frequency approximation, see (42), while the α in (37) stems from a low-frequency approximation. The answer to this paradox is that there is an overlap in the respective regions of validity. To specify this overlap region, one must now find the lower limit of Ω corresponding to (42), for which (2) and (3) are still valid.

The low-frequency limit of the expressions in (2) and (3) for α and β can be examined more precisely with the help of the asymptotic expressions for the conductor surface impedance Z_s. An expression for $\gamma^2=(\alpha+j\beta)^2$, valid down to zero frequency, can be obtained from Morgan's paper[3] (see page 894, formula 41). It is

$$\gamma^2 = -\omega^2\epsilon\mu + j\omega\sqrt{\epsilon\mu}\,\frac{(1/\rho_1+1/\rho_2)Z_s}{\sqrt{\frac{\mu}{\epsilon}}\ln(\rho_2/\rho_1)}. \tag{44}$$

Using (28) one can write this in the form

$$\gamma^2 = -\omega^2\epsilon\mu\left\{1+\frac{2Z_s}{j\omega\mu\rho}\right\}, \tag{45}$$

illustrating the deviation in γ^2 from free-space propagation conditions. One may now apply (34) and (20); (45) then becomes

$$\gamma^2 \approx -\omega^2\epsilon\mu\left\{1+\frac{4t}{j\Omega\rho}\right\}. \tag{46}$$

The first two terms in the binomial expansion of the square root of (46) are adequate for justifying (2) and (3) only if

$$\Omega \gg \frac{t}{\rho}. \tag{47}$$

The ratio t/ρ is very small; for example, $t=10^{-5}$ m and $\rho=10^{-3}$ m gives $t/\rho=10^{-2}$. Hence, $\Omega=10^{-1}$ should be an acceptable lower limit for Ω. Eq. (47) represents a more explicit form of Morgan's requirement (formula 42).[3]

Conclusion

The thin conductor coaxial transmission line has been discussed from a theoretical point of view with somewhat more detail than customary, leading to the conclusion that this line gives a substantially improved phase and attenuation over a reduced frequency range of approximately $0.1<\Omega<10$ with $\Omega=2\mu\ \sigma\omega t^2$ [see (20)]. For $\Omega>10$, the thin conductor line approaches the behavior of the solid conductor line; for $\Omega<0.1$, the quality of the line deteriorates depending on how small the thickness t of the conductor is with respect to the cross-sectional dimensions of the line. The characteristic impedance in the interval $0.1<\Omega<10$ can very nearly be represented by a resistance in series with a capacitance of value indicated by (39).

These theoretical results depend on a rather complex chain of simplifying engineering assumptions which really need some further experimental justification. The attenuation expressions are reasonably well supported by experiment. No separate and direct experimental evidence exists for the improved linearity of the phase response. Some preliminary experiments at Bell Telephone Laboratories on an available cable sample provided an indirect proof that the phase distortion is reduced, because pulse response on the thin conductor cable is considerably better than on its solid conductor counterpart.

In this connection it is important that the approximate phase and attenuation expressions in (29) can be shown to satisfy the criterion of physical compatibility; that is, they cannot lead to a response prior to the time of initiation of the input signal plus, at least, the empty space delay time corresponding to the length of the line. This criterion is also met by the expressions in (33) for the solid conductor line. This holds even though the expressions for either case are known not to be valid for the entire frequency range from zero to infinity. A justification of these statements would require a detailed argument that does not fall within the scope of this report. Note that it is frequently assumed that small nonlinear phase components can be ignored with respect to the linear delay component; for example, the $\sqrt{\Omega}$ term with respect to ω in (35). This approximation does not satisfy the physical compatibility criterion and thus leads to physically impossible transient responses.

Acknowledgment

Approximately two thirds of the work reported in this paper was performed while the author was a member of the technical staff of Bell Telephone Laboratories, Murray Hill, N. J. The author would like to acknowledge important help he received from other members of that organization: L. O. Schott provided the initial stimulation and assisted the author throughout with his active interest; A. Pal made the computations for Figs. 4 and 5, and A. J. Rack, G. A. Backman, and A. F. Dietrich provided the experimental data referred to in the Conclusion; finally, we would like to acknowledge the comments of Dr. G. Raisbeck, S. E. Miller, and Dr. B. G. King's checking of some of the equations.